AGU PUBLICATIONS

Water Resources Research

RESEARCH ARTICLE

10.1002/2017WR020576

Key Points:

- Hyporheic flow paths do not respond uniformly to different stream discharge and groundwater inflow conditions
- Hyporheic flow paths with hydraulic gradients similar to the valley gradient are the most sensitive to changing hydrologic conditions
- Hyporheic flow paths with hydraulic gradients set by large morphologic features are the least sensitive to changing hydrologic conditions

Supporting Information:

- Supporting Information S1

Correspondence to:
N. M. Schmadel,
nschmadel@gmail.com

Citation:
Schmadel, N. M., A. S. Ward, and S. M. Wondzell (2017), Hydrologic controls on hyporheic exchange in a headwater mountain stream, *Water Resour. Res.*, *53*, 6260–6278, doi:10.1002/2017WR020576.

Received 11 FEB 2017
Accepted 29 JUN 2017
Accepted article online 6 JUL 2017
Published online 31 JUL 2017

Hydrologic controls on hyporheic exchange in a headwater mountain stream

Noah M. Schmadel[1], Adam S. Ward[1], and Steven M. Wondzell[2]

[1]School of Public and Environmental Affairs, Indiana University, Bloomington, Indiana, USA, [2]Pacific Northwest Research Station, Forest Service, United States Department of Agriculture, Corvallis, Oregon, USA

Abstract The spatial and temporal scales of hyporheic exchange within the stream corridor are controlled by stream discharge and groundwater inflow interacting with streambed morphology. While decades of study have resulted in a clear understanding of how morphologic form controls hyporheic exchange at the feature scale, we lack comparable predictive power related to stream discharge and the spatial structure of groundwater inflows at the reach scale, where spatial heterogeneity in both geomorphic setting and hydrologic forcing are present. In this study, we simulated vertical hyporheic exchange along a 600 m mountain stream reach under high, medium, and low stream discharge while considering groundwater inflow as negligible, spatially uniform, or proportional to upslope accumulated area. Most changes to hyporheic flow path residence time or length in response to stream discharge were small ($<$5%), suggesting that discharge is a secondary control relative to morphologically driven hyporheic exchange. Groundwater inflow was a primary control and mostly caused decreases in hyporheic flow path residence time and length. This finding generally agrees with expectations from the literature; however, flow path response was not consistent across the study reach. Instead, we found that flow paths driven by large hydraulic gradients coinciding with large morphologic features were less sensitive to changes in groundwater inflow than those driven by hydraulic gradients similar to the valley gradient. Our results indicate that consideration of heterogeneous arrangement of morphologic features is necessary to differentiate between hyporheic flow paths that persist in time and those that are sensitive to changing hydrologic conditions.

1. Introduction

Accurate prediction of downstream transport of water, solutes, energy, and materials requires a holistic representation of exchange between the stream, riparian aquifer, hillslope, and groundwater—collectively termed the "river or stream corridor" [*Harvey and Gooseff*, 2015]. Within the stream corridor, the exchange of water between streams and their valleys through hyporheic flow paths underpins a host of water quality benefits and other ecosystem services [e.g., *Boano et al*., 2014; *Buffington and Tonina*, 2009]. The extent and distribution of hyporheic flow paths are primarily controlled by interactions between hydrologic forcing (e.g., stream discharge and groundwater inflow) and geomorphic setting (e.g., streambed form and planform morphology) [e.g., *Boano et al*., 2007; *Ward et al*., 2012]. At the morphologic-feature scale (or channel-unit scale), interactions between the flowing stream and individual features (e.g., a bed form, meander, or step-pool sequence) create pressure gradients that induce hyporheic flow paths [e.g., *Tonina and Buffington*, 2009, 2011]. While these interactions often drive hyporheic exchange both laterally [e.g., *Francis et al*., 2010; *Gerecht et al*., 2011; *Stonedahl et al*., 2010] and vertically [e.g., *Precht and Huettel*, 2003; *Sawyer et al*., 2013], streambed morphologic features are typically recognized as the dominant control on vertical hyporheic exchange [*Gomez-Velez and Harvey*, 2014; *Gomez-Velez et al*., 2015]. Yet we lack comparable predictive power across changing hydrologic conditions.

In response to seasonal (e.g., snow-melt periods) or individual hydrologic events (e.g., storms), increases in stream discharge and stage are commonly attributed in part to corresponding increases in groundwater inflows to the stream corridor. An increase in stream discharge has been reported to decrease the role of individual features by causing the down-valley hydraulic gradient to become more uniform [*Church and Zimmermann*, 2007; *Dunne and Leopold*, 1978; *Ward et al*., 2016], but the increase in stage may force additional exchange across the streambed [*Boano et al*., 2013; *Hassan et al*., 2015; *Trauth et al*., 2015].

While this contradiction indicates that the influence of stream discharge may not be consistent across valley settings, an increase in groundwater inflow has been shown to almost exclusively decrease the extent of hyporheic exchange driven by streambed features [*Boano et al*., 2008; *Cardenas and Wilson*, 2007a; *Gomez-Velez et al*., 2015]. Altogether, decades of study have yielded predictive relationships at the scale of individual morphologic features. However, these individual features are recognized to represent one spatial scale of a nested system; interactions at both smaller and larger scales are expected to complicate exchange processes [e.g., *Stonedahl et al*., 2013, 2010; *Wörman et al*., 2007]. It remains unknown if the expected relationships between stream discharge and groundwater inflow that influence hyporheic exchange hold at the scale of stream reaches, where the heterogeneous arrangement of channel-unit scale morphologic features and hydrologic controls interact at larger scales, potentially causing nonuniform effects on hyporheic exchange.

Predictive relationships between steady hydrologic and morphologic interactions have enabled upscaling physical and biogeochemical processes to entire basins [*Gomez-Velez and Harvey*, 2014; *Gomez-Velez et al*., 2015; *Kiel and Cardenas*, 2014]. An implicit assumption about these relationships is that feature-scale processes are additive to form reaches, and these reaches are additive to form networks (i.e., aggregated features adequately represent the heterogeneity of a network), which is appropriate if there is a single scale and type of feature that is the dominant driver of hyporheic exchange. However, the robustness of this assumption is uncertain across hydrologic conditions and valley settings because local hyporheic flow path distributions are nested within larger reach-scale down-valley flow and catchment-scale groundwater flow [e.g., *Boano et al*., 2007; *Ward et al*., 2013b], and the interactions within these nested scales remain unstudied. For example, when the arrangement of morphologic features is heterogeneous and the down-valley and groundwater flow field is continuous, each feature may impact its neighbor differently under changing stream discharge conditions, potentially causing spatially variable responses to the hyporheic flow field [e.g., *Dudley-Southern and Binley*, 2015; *Zimmer and Lautz*, 2014]. Furthermore, these upscaling relationships are modeled after large, low-gradient alluvial river corridors less confined by their valleys where bed forms and high sinuosity are common [e.g., *Gomez-Velez et al*., 2015]. In contrast, stream networks in mountainous catchments are characterized by network expansion and contraction due to different hydrologic periods (e.g., seasonal changes) [e.g., *Godsey and Kirchner*, 2014; *Jencso et al*., 2010, 2009]. In such confined mountainous valley settings, subsurface down-valley flow can represent a large portion of persistent flow paths [*Castro and Hornberger*, 1991; *Jackman et al*., 1984; *Ward et al*., 2013b], possibly explaining why order-of-magnitude changes in stream discharge have been shown to have inconsequential impact on hyporheic exchange [e.g., *Ward et al*., 2014, 2016, 2017]. Groundwater inflow driven by mountainous catchment topology (e.g., hillslope inputs as a function of lateral area), however, can cause spatial fragmentation of the hyporheic flow field [*Caruso et al*., 2016]. Given that mountainous stream networks are so different than their lower-gradient counterparts, we sought to improve understanding of the hydrologic factors that control hyporheic exchange in headwater mountain streams to provide a basis to upscale from features to networks.

Whereas past studies have focused on simplified morphology (e.g., individual meander bends or bed forms) and hydrology (e.g., uniform groundwater inflows), the findings of these studies have not been extended to the reach scale where heterogeneity in both morphologic and hydrologic controls generate a complex mosaic of exchange pathways. Thus, we address the following question: how do spatially heterogeneous hydrologic forcing (stream stage and groundwater inflow) interact with spatially heterogeneous morphology to control reach-scale hyporheic exchange in confined mountainous stream corridors? We hypothesize that all hyporheic flow paths will respond uniformly to different stream discharge and groundwater inflow conditions, as is assumed by emerging upscaling models. To answer our research question, we focus on a mountainous stream corridor that is bedrock constrained, confined by steep hillslopes, and predominantly step-pool morphology. To test our hypothesis, we simulated vertical groundwater flow through the stream corridor at the thalweg during three different steady discharge conditions. For each stream discharge, we considered groundwater inflow as negligible, as spatially uniform, and as a function of upslope accumulated area. We compared distributions of hyporheic exchange flux, flow path residence time, and flow path length across the three stream discharge conditions for each groundwater inflow case. Through these comparisons, we determined how hyporheic flow paths across a reach respond to these different hydrologic conditions.

2. Methods

2.1. Site Description and Data Collection

The stream corridor study reach encompasses approximately 600 m of the valley of Watershed 1 (WS01), a headwater catchment in the H. J. Andrews Experimental Forest (HJA) in the western Cascades, Oregon, USA (Figure 1a). This study reach is bound by distinct bedrock outcrops at the upstream and downstream extents, and at one intermediate location, allowing explicit model boundaries to be set [after *Ward et al.*, 2013a]. The streambed is primarily step-pool morphology. The catchment is gaged for stream discharge with a flume and weir calibrated and maintained by the U.S. Forest Service. The catchment is highly dissected and characterized by steep hillslopes (>50%) and a confined, steep valley bottom (~12%). The colluvium in the valley bottom consists of a poorly sorted mix of boulders, logs, cobbles, gravels, sands, and finer sediments (see *Wondzell* [2006] and *Voltz et al.* [2013] for more details regarding site characteristics).

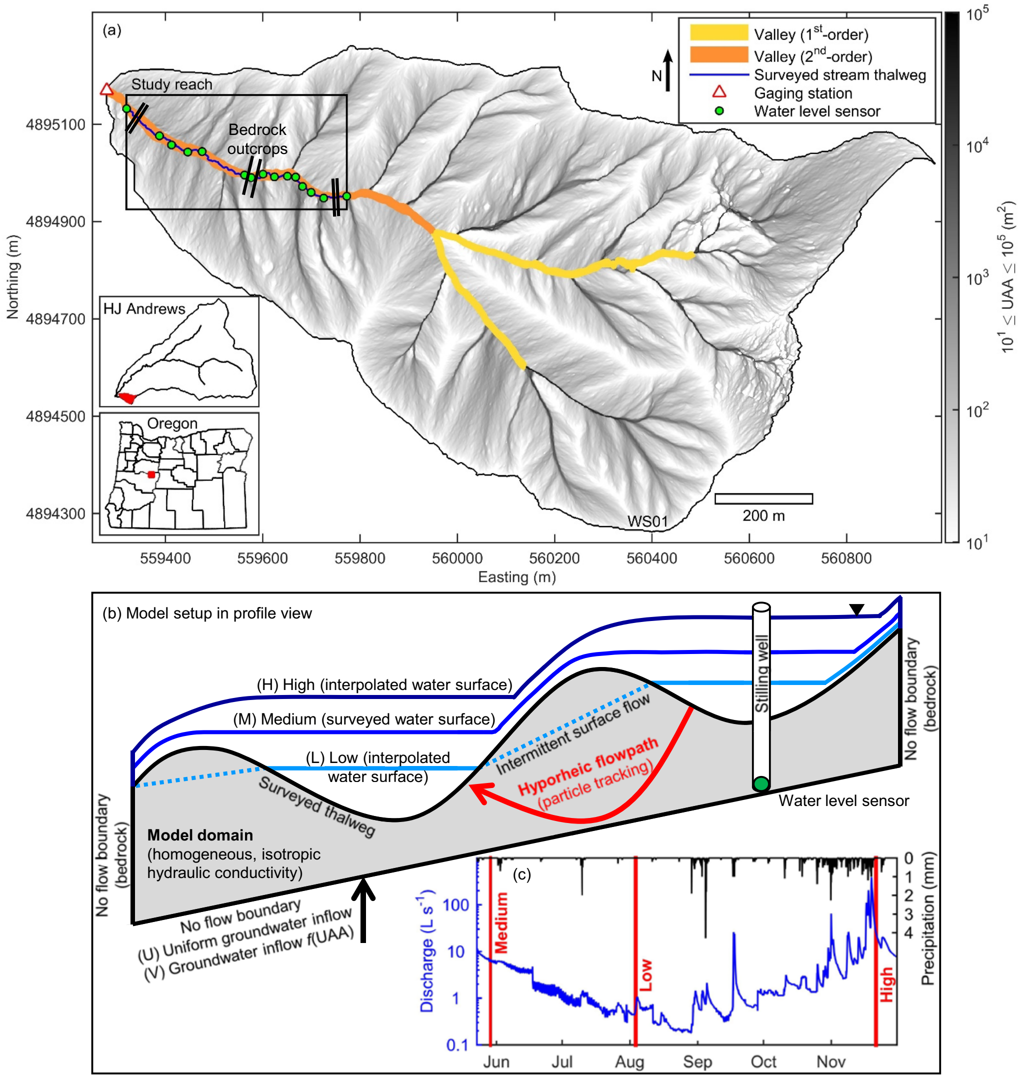

Figure 1. (a) Upslope accumulated area (UAA) and approximate first-order and second-order valley bottoms of Watershed 1 (WS01) in the H. J. Andrews Experimental Forest in the western Cascades, Oregon. The 96 ha catchment is gaged for stream discharge. The study reach includes a topographically surveyed stream thalweg and water surface, and 15 sensors recording continuous water level. (b) Model setup (not to scale) and boundary conditions of steady, two-dimensional, vertical groundwater flow. The top boundary (streambed interface) was set as three conditions: high (H), medium (M), and low (L) stream discharge. The bottom boundary was also set as three different conditions: no flow boundary, uniform groundwater inflow (U), and spatially variable groundwater inflow (V) as a function of UAA, resulting in nine possible hydrologic cases (see Table 1). Mass less particles were released at the streambed boundary and tracked to estimate hyporheic flow path residence time and length. (c) Stream discharge at the gaging station and local precipitation. The high, medium, and low stream discharge periods in 2015 coincide with no precipitation.

Using a 1 m digital terrain model dated August 2008 [*Spies*, 2016], upslope accumulated area (UAA) of hillslopes within the catchment were estimated [after *Schwanghart and Kuhn*, 2010; *Seibert and McGlynn*, 2007]. The catchment is relatively small with a total area of about 96 ha. The valley bottom width was measured at 30 locations throughout the study reach, providing a mean valley bottom width of 10.6 m (range 2.6–16.8 m).

A detailed topographic survey of the streambed along the thalweg and water surface profile in the study reach was conducted using a Trimble S6 Robotic Total Station 26–29 May 2015. The upstream-most 70 m, completed 26 May 2016, during similar stream discharge conditions, was added to extend the detailed survey upstream to the next distinct bedrock outcrop that serves as an upper boundary condition in our model. There were no visible changes in morphology between the two surveys. Water level sensors (HOBO Water Level Data Logger U20L-04 and U20–001-04, Onset, Bourne, MA) were placed at the bottom of stilling wells installed in the stream at 15 locations (Figure 1a). These sensors measured continuous absolute pressure, which were corrected to barometric pressure measured near the downstream end of the study reach. A linear elevation correction was applied to the barometric pressure to estimate stream stage relative to the streambed at every stilling well location. Stream stage was manually measured three times (26–29 May during the time of installation, 21 November 2015, and 23 May 2016) to corroborate the elevation corrected stage. The sensors were installed below the underlying bedrock surface (5 sensors) or deep into the colluvium (10 sensors) to ensure that they remained submerged during low stream discharge conditions. Although each sensor remained submerged, the stream did become spatially intermittent during the low discharge period based on visual inspection of the site and recorded stages relative to the streambed.

2.2. Stream Discharge and Groundwater Inflow as Controls on Hyporheic Exchange

2.2.1. Model Setup and Data-Driven Boundary Conditions

We constructed a two-dimensional, finite element model of steady groundwater flow through the valley bottom in the vertical profile (Figure 1b). While the model setup is based on site-specific information and observations, it is not calibrated to the site. Rather, the model is heuristic; simulations were constructed to identify patterns in hyporheic flow path response due to different hydrologic boundary conditions and to test our hypothesis, which is consistent with common practice [e.g., *Cardenas and Wilson*, 2007b; *Gooseff et al.*, 2006; *Irvine and Lautz*, 2015; *Malzone et al.*, 2016; *Schmadel et al.*, 2016; *Trauth et al.*, 2013]. Richards' equation was used to allow for groundwater flow simulations through the valley bottom for all possible hydrologic conditions ranging from a fully saturated subsurface to some locations of unsaturated subsurface [*Richards*, 1931],

$$\frac{\partial}{\partial x}\left[K(h)\frac{\partial h}{\partial x}\right]+\frac{\partial}{\partial z}\left[K(h)\left(\frac{\partial h}{\partial z}+1\right)\right]=0, \tag{1}$$

where $h(x,z)$ is the hydraulic head (m), x is the stream-wise (down-valley) direction (m), z is the vertical direction (m), and $K(h)$ is the unsaturated hydraulic conductivity when h is less than the streambed elevation (m s^{-1}). During spatially variable unsaturated groundwater flow, we used the *Mualem* [1976] and *van Genuchten* [1980] retention model,

$$K(h)=K_s S_e{}^{l}\left[1-\left(1-S_e{}^{1/m}\right)^{m}\right]^2, \tag{2}$$

$$S_e=\frac{\theta(h)-\theta_r}{\theta_s-\theta_r}=\left(1+|\alpha h|^{n}\right)^{-m}, \tag{3}$$

where K_s is the saturated homogeneous, isotropic hydraulic conductivity (m s^{-1}), S_e is the effective water saturation ($0 \le S_e \le 1$), θ_s is the saturated water content (equivalent to the effective porosity), θ_r is the residual water content, α is related to mean pore size (m^{-1}), n is an empirical constant dependent on soil type, $m = 1 - 1/n$, and l is the tortuosity coefficient. Specific discharges were estimated using Darcy's law,

$$q_x=-K(h)\frac{\partial h}{\partial x},\ q_z=-K(h)\frac{\partial h}{\partial z} \tag{4}$$

For fully saturated groundwater flow, $K = K_s$ and equation (1) simplifies to the Laplace equation. COMSOL Multiphysics was used to solve equation (1) and implement particle tracking (described below). The model domain is made up of 17,971 triangular elements with an average area of 0.08 m^2.

A K_s of 7×10^{-5} m s^{-1} and effective porosity of 0.2 for poorly sorted colluvium were used after *Wondzell et al*. [2009]. This K_s is the geometric mean of falling-head tests performed in WS01 and a neighboring headwater catchment [*Kasahara and Wondzell*, 2003]. Although application of Richards' equation is more typical for silts, clays, and sands [*Richards*, 1931], it has been successfully applied at regional scales [*Botros et al*., 2009; *Downer and Ogden*, 2004] and found valid for some coarser sediments of poorly sorted sands and gravels [*El-Kadi*, 2005]. We use Richards' equation for our study reach because it is the simplest and most broadly used method for simulating unsaturated groundwater flow conditions. Higher α and lower θ_r values are consistent with coarser material, which results in more rapid responses in S_e and K due to varying h. To generally represent the characteristics of the study reach, we set $\alpha = 5$ m^{-1}, $\theta_r = 0.05$, $n = 2.5$ [similar to *El-Kadi*, 2005], and $l = 0.5$ based on the observed K_s [after *Carey et al*., 2016]. While we assume that Richards' equation is appropriate for our study reach where spaces between cobbles, boulders, and logs are filled with fine sediment, we note that it may be less suitable in media with large pore spaces such as coarse gravels, which could limit the ability for a numerical solution to converge [*Niswonger and Prudic*, 2004].

The depth of the colluvium was set to an average 3 m for a second-order stream based on similar modeling studies conducted on different stream orders at the HJA [*Gooseff et al*., 2006]. Underlying bedrock was treated as a planar surface after *Wondzell et al*. [2009] who found little influence of incorporating bedrock topography on groundwater flow simulations in WS01.

In steep headwater mountain streams with step-pool morphology, hydrostatic gradients are expected to be the dominant driver of hyporheic exchange, in contrast to low-gradient rivers where bed form pumping or turbulent momentum diffusion into the streambed (hydrodynamic contribution) are more influential mechanisms [e.g., *Boano et al*., 2014; *Wondzell and Gooseff*, 2013]. Momentum diffusion has been found to influence only the first ~5 cm of the hyporheic zone depth [*Packman et al*., 2004]. Although an increase in the stream Reynolds number can increase the diffusion depth and possibly warrant a coupled Navier-Stokes and Brinkman-Darcy approach, most of the momentum still dissipates within a shallow depth, even during conditions of high stream turbulence [*Malzone et al*., 2016]. Therefore, the streambed boundary was set to hydrostatic head due to the water level relative to the streambed, and we ignore hydrodynamic contributions. The streambed boundary condition was set during three different stream discharge conditions: high (25 L s^{-1}, 21 November 2015), medium (7 L s^{-1}, mean discharge of the 26–29 May 2015, topographic survey period), and low (0.6 L s^{-1}, 3 August 2015) (Figure 1c). The selected discharge periods were free from precipitation (Figure 1c). We assume inputs to the valley bottom were only subsurface discharge from the hillslopes, as the site is known to seldom generate overland flow contributions to the stream channel [*Amatya et al*., 2016]. The study reach was visually observed during these time periods to corroborate either no overland surface flows or spatial intermittency in the stream. We developed continuous water surface profiles for the high and low stream discharge conditions using the water level sensors and the water surface profile surveyed during the medium stream discharge period. We calculated deviations from the surveyed profile according to the water level sensors at each stilling well, linearly interpolating deviations between the water level sensors, and adjusting the surveyed profile based on these interpolated deviations.

We assume that the stream corridor study reach has no losses to deeper aquifers given the known underlying bedrock and visual bedrock outcrops. Groundwater inflow to the valley bottom was estimated based on UAA and stream discharge. We first estimated the ratio, *R*, of stream discharge to UAA assuming a linear relationship,

$$R(t) = \frac{Q(t)}{UAA_{\max}}, \tag{5}$$

where $Q(t)$ is the stream discharge reported at the gaging station (m^3 s^{-1}), *t* is the time of the selected discharge period (Figure 1c), and UAA_{max} is the UAA of the entire catchment with the gaging station as the outlet (96 ha). Next, we estimated the total upstream, Q_{up} (m^3 s^{-1}), and downstream, Q_{down} (m^3 s^{-1}), discharge through the stream corridor at the study reach limits,

$$Q_{down}(t) = R(t) UAA_{down}, \tag{6}$$

$$Q_{up}(t) = R(t) UAA_{up}, \tag{7}$$

where UAA_{down} is the UAA at the downstream reach limit (m^2) and UAA_{up} is the UAA at the upstream reach limit (m^2). A single-direction flow routing algorithm was used to estimate UAA_{down} and UAA_{up} [*Schwanghart*

Table 1. Summary of Model Runs for Each Hydrologic Case and Associated Conditions

Stream Discharge Condition	Spatial Groundwater Inflow Condition	Model Run and Case	Stream Discharge at Upstream Reach Limit (L s^{-1})	Stream Discharge at Downstream Reach Limit (L s^{-1})	Total Hillslope Contribution to Study Reach (L s^{-1})	Mean Upward Groundwater Flux (m s^{-1})	Stream Discharge at Gage (L s^{-1})	Stream Water Surface Profile
High	None	H	25.0	25.0	0	0	25.0	Interpolated between 15 sensors
	Uniform	HU	19.2	24.8	5.6	9.1E-07		
	Variable	HV	19.2	24.8	5.6	9.5E-07		
Medium	None	M	7.0	7.0	0	0	7.0	Topographic survey
	Uniform	MU	5.4	6.9	1.5	2.6E-07		
	Variable	MV	5.4	6.9	1.5	2.7E-07		
Low	None	L	0.6	0.6	0	0	0.6	Interpolated between 15 sensors
	Uniform	LU	0.46	0.59	0.13	2.2E-08		
	Variable	LV	0.46	0.59	0.13	2.3E-08		

and Kuhn, 2010; *Tarboton*, 1997]. The total discharge contribution from the hillslope, Q_{hs} (m^3 s^{-1}), was estimated,

$$Q_{hs}(t) = Q_{down}(t) - Q_{up}(t). \tag{8}$$

Finally, we estimated the upward velocity of groundwater inflow, u_{gw} (m s^{-1}),

$$u_{gw}(t) = \frac{Q_{hs}(t)}{\bar{B}_{valley} L}, \tag{9}$$

where $\bar{B}_{valley}$ is the mean valley bottom width (m) and L is the length of the study reach (m). Equation (9) provides an estimate of the upward groundwater velocity uniformly distributed across the study reach (uniform groundwater inflow). To estimate spatially variable groundwater inflow velocity, v_{gw} (m s^{-1})—that more closely reflects catchment topology—we estimated Q_{down} and Q_{up} every 1 m, which are based on corresponding 1 m estimates of UAA_{down} and UAA_{up} (see equations (6) and (7)),

$$v_{gw}(x,t) = \frac{Q_{hs}(x,t)}{\bar{B}_{valley} \Delta L}, \tag{10}$$

where ΔL is the length between Q_{up} and Q_{down} (~1 m in this case). See Table 1 and supporting information Figure S1 for uniform and spatially variable groundwater inflow velocities during the high, medium, and low stream discharge conditions. Stream discharge and UAA estimates are consistent with recent work done in the catchment [*Corson-Rikert et al.*, 2016].

For each hydrologic case (section 2.2.2 and Table 1), mass less particles were released at the streambed boundary every 10 cm and tracked through the subsurface model domain. Particle tracking was implemented in COMSOL where each particle release produced a unique track. Particles that infiltrated the subsurface in downwelling (negative vertical flux) zones and returned to the stream were considered hyporheic flow paths (Figure 1b). All flow paths that downwelled returned to the stream because the study reach is constrained by bedrock outcrops that span the full width of the valley floor, which were set as no flow boundaries. To focus only on hyporheic flow paths, groundwater flow paths originating at the bottom boundary were simulated but not tracked. For the low stream discharge condition, we did not release nor track particles at any location where the streambed was dry (i.e., all down-valley flow was subsurface). Particle velocities (pore water velocities) were estimated by dividing the specific discharges (equation (4)) by the effective porosity [e.g., *Sawyer et al.*, 2009; *Schmadel et al.*, 2016; *Stonedahl et al.*, 2013]. The time elapsed from particle release to return to the stream was tabulated and represents the hyporheic flow path residence time. Flow path lengths and vertical downwelling fluxes at the particle release locations were also tabulated. We did not weight the flow path residence times by flux because we are not constructing reach-scale stream residence time probability density functions. Instead, our distributions represent the subsurface flow paths themselves [after *Ward et al.*, 2011]. Flux-weighting residence times would be important if objectives of the research were centered on the impact of hyporheic exchange on in stream processes or across different spatial scales such as by *Gomez-Velez et al.* [2015]. However, our focus in this study is on the spatial and temporal scales of the hyporheic flow paths themselves, not on their aggregate impact on the stream. Thus, we use non-weighted flow path distributions to isolate those flow paths that are most likely to change in response to changing hydrologic conditions [e.g., *Kasahara and Wondzell*, 2003; *Schmadel et al*., 2016; *Ward et al*., 2011; *Wondzell et al*., 2009]. Therefore, changes to the stream corridor due to different hydrologic conditions are described by the downwelling flux and by the hyporheic flow path residence time and length.

2.2.2. Comparisons of Hydrologic Cases

All comparisons of hydrologic cases were performed to isolate stream discharge and groundwater inflow as controls on hyporheic flow path residence times, lengths, and downwelling fluxes. We simulated nine possible combinations of high, medium, and low stream discharge (H, M, L) each with no, spatially uniform, and spatially variable groundwater inflows (no, U, V; Table 1).

We calculated summary statistics including the median, mean, maximum, variance, coefficient of variation, and skewness of the reach-scale distributions of downwelling flux (m d^{-1}), hyporheic flow path residence time (h), and hyporheic flow path length (m) for each of the nine hydrologic cases. We compared case-specific, reach-scale distributions with a Kruskal-Wallis one-way analysis of variance (ANOVA) to investigate the integrated, reach-scale response to the different hydrologic conditions. We selected this test to prevent introducing bias because the test does not assume normally distributed error or constant variance as is the case with a standard one-way ANOVA. A resulting p value < 0.05 specifies medians between two distributions are significantly different. To isolate stream discharge as a control, we compared H to M (H:M), H to L (H:L), and M to L (M:L). To isolate groundwater inflow as a control, we compared H:HU, H:HV, M:MU, M:MV, L:LU, and L:LV. We also compared HU:HV, MU:MV, and LU:LV to determine if the representation of groundwater inflow as uniform or spatially variable had an impact on the reach-scale response of hyporheic flow paths. Significant differences between uniform and spatially variable distributions would indicate that larger, catchment-scale topology is an important control on groundwater inflow and, in turn, an important control on hyporheic flow paths.

In addition to analyzing the integrated, reach-scale response, we calculated changes in the residence time, length, and downwelling flux associated with each individual flow path in response to different stream discharge and groundwater inflow conditions. These changes were quantified as a percent increase or decrease from the associated baseline case. We estimate change in each individual flow path to better examine hydrologic controls on hyporheic exchange across a reach with realistic arrangement of morphologic features rather than focus on the response across any single feature. To isolate stream discharge as a control, we treated M as the baseline case and examined the change as discharge increased (H-M) and decreased (L-M). To isolate groundwater inflow as a control, we examined the change relative to H as the baseline (HU-H and HV-H), M as the baseline (MU-M and MV-M), and L as the baseline (LU-L and LV-L). We assume that a flow path change must result from one (or a combination) of the following three options: (1) the flow path is deactivated (switches from downwelling to upwelling or the stream becomes spatially intermittent); (2) the flow path is truncated or extended with the particle exiting the model domain at a different location; or (3) the flow path has no change in shape or exiting location but the velocity changes, thereby changing the residence time. Therefore, of the flow paths that changed, we tabulated the residence times, lengths, and downwelling fluxes corresponding to the baseline case to provide an indication as to which flow paths were most sensitive to a change in stream discharge or groundwater inflow. A Kruskal-Wallis one-way ANOVA was performed to determine if some suites of baseline flow paths were more prone to increases or decreases in response to the different hydrologic conditions. Following these comparisons, we further examined which baseline flow paths may be more sensitive to stream discharge or groundwater inflow by defining major changes as those that increased or decreased more than 5%. We applied a Kruskal-Wallis one-way ANOVA to determine if baseline flow paths that persisted (change $<5\%$), increased, or decreased were significantly different.

3. Results

3.1. Reach-Scale Responses to Different Stream Discharges and Groundwater Inflows

3.1.1. Stream Discharge as a Control

Stream discharge was not a primary control on reach-scale distributions of hyporheic flow path residence times during periods of spatially continuous stream discharge conditions (Figure 2). There was no significant difference in flow path residence time distributions between high (H) and medium (M) stream discharge conditions with no groundwater inflow (H:M $p = 0.989$; Table 2). When the stream discharge was low

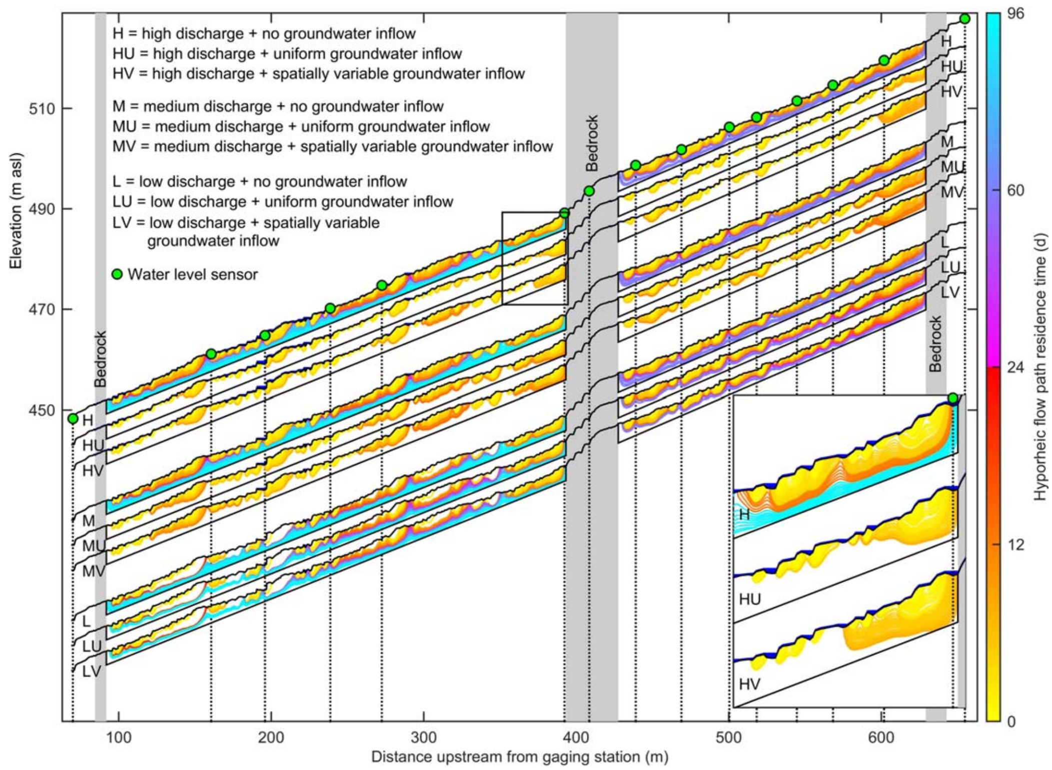

Figure 2. Particle tracking simulations and hyporheic flow path residence times for nine possible combinations of high, medium, and low stream discharge (H, M, L) with no, spatially uniform, and spatially variable groundwater inflows (no, U, V; see Table 1). Locations of water level sensors and bedrock outcrops are indicated. See supporting information Figures S2 and S3 for flow path lengths and fluxes.

enough to cause spatial intermittency in surface flow (i.e., during the low stream discharge with no groundwater inflow (L) case), there was a significant change in the reach-scale hyporheic flow path residence time distribution (H:L $p = 0.013$ and M:L $p = 0.013$; Table 2). During the L case, some hyporheic flow paths were deactivated due to spatial intermittency (from H to L, 33% of the flow paths were deactivated, Table 3). Summary statistics (median, mean, maximum, variance, coefficient of variation, and skewness) for H and M were similar, while L had longer reach-average residence times than H and M (Table 3). However, L had a similar coefficient of variation and lower skewness compared to H and M. A similar pattern was found for reach-average lengths (supporting information Table S1), but there was little change in summary statistics of downwelling fluxes across different stream discharges (supporting information Table S2).

Table 2. Comparisons of Reach-Scale Hyporheic Flow Path Residence Time Distributions of the Hydrologic Cases (See Table 1)[a]

Hyporheic Flow Path Residence Time			
Stream Discharge as a Control			
Comparison	H:M	H:L	M:L
p	0.989	**0.013**	**0.013**
Groundwater Inflow as a Control During High Stream Discharge			
Comparison	H:HU	H:HV	HU:HV
p	**1.9E-11**	**4.8E-06**	**0.030**
Groundwater Inflow as a Control During Medium Stream Discharge			
Comparison	M:MU	M:MV	MU:MV
p	**0.020**	**0.046**	0.769
Groundwater Inflow as a Control During Low Stream Discharge			
Comparison	L:LU	L:LV	LU:LV
p	0.795	0.820	0.985

[a]Bold indicates significant value. A p value < 0.05 indicates the medians of the two corresponding distributions are statistically different. See supporting information Tables S1 and S2 for flow path length and flux comparisons.

Significant differences in reach-scale residence time distributions between spatially continuous and spatially intermittent stream discharge are due to a combination of changing flow path lengths, changing downwelling fluxes, and deactivation of flow paths. Hyporheic flow path lengths responded similarly to stream discharge as did the flow path residence times ($p = 0.888$ for H:M, $p = 0.011$ for H:L, and $p = 0.016$ for M:L comparisons; supporting information Table S1 and Figure S2). A change in stream discharge did not have a significant

Table 3. Reach-Scale Summary Statistics of Hyporheic Flow Path Residence Times for Each Hydrologic Case (See Table 1)[a]

	Hyporheic Flow Path Residence Time								
	High Stream Discharge			Medium Stream Discharge			Low Stream Discharge		
Summary Statistic	H	HU	HV	M	MU	MV	L	LU	LV
Number of flow paths	3188	2943	2912	3180	3080	3099	2139	2133	2135
% deactivated from H		7.7	8.7	0.3	3.4	2.8	32.9	33.1	33.0
Median (h)	9.3	7.1	7.7	9.2	8.4	8.5	11.2	11.1	11.1
Mean (h)	57.9	17.5	22.2	56.9	26.3	28.4	68.7	55.8	57.7
Maximum (h)	2296.4	192.2	288.4	2313.9	327.3	320.0	2296.5	2285.2	2274.3
Variance (h^2)	44173.1	677.7	1369.0	44230.6	2052.3	2537.2	58314.3	31197.9	34999.2
Coefficient of variation	3.6	1.5	1.7	3.7	1.7	1.8	3.5	3.2	3.2
Skewness	7.8	2.7	3.1	8.1	3.2	3.0	6.9	7.9	7.7

[a]See supporting information Tables S1 and S2 for summary statistics of the flow path lengths and fluxes.

impact on downwelling fluxes across the entire study reach ($p > 0.05$ for H:M, H:L, and M:L comparisons; supporting information Table S2 and Figure S3).

3.1.2. Groundwater Inflow as a Control

Groundwater inflow was a primary control on reach-scale distributions of hyporheic flow path residence times only during periods of spatially continuous stream discharge conditions. There was a general reduction in the longest residence time flow paths for both uniform and spatially variable groundwater inflow cases (HU, HV, MU, and MV; Figure 2). During high stream discharge, groundwater inflow caused an overall reduction in hyporheic flow path residence times for both uniform and spatially variable representations (H:HU and H:HV $p \ll 0.001$ and up to a 9% reduction in the number of flow paths when groundwater inflow was considered; Tables 2 and 3). The coefficient of variation was reduced by up to 60% and skewness was reduced by 65%, indicating groundwater inflow substantially reduced the amount of longer residence time flow paths. There was also a significant difference between residence times across the study reach due to the representation of groundwater inflow as uniform or spatially variable (HU:HV $p = 0.030$; Table 2). During medium stream discharge, both uniform and spatially variable groundwater inflow had a significant impact on flow path residence times (M:MU $p = 0.020$, M:MV $p = 0.046$, and a 3% reduction in the number of flow paths; Tables 2 and 3). In contrast to high stream discharge, there was no significant difference between uniform and spatially variable representations during medium stream discharge (MU:MV $p = 0.769$; Table 2). Groundwater inflow was so small during low stream discharge (LU and LV) that the reach-scale distribution of flow path residence times was not significantly affected by the presence of groundwater inflow (L:LU, L:LV, and LU:LV $p \gg 0.05$; Table 2).

The influence of groundwater inflow on hyporheic flow path lengths at the reach scale followed a pattern similar to flow path residence times (supporting information Table S1 and Figure S2). Groundwater inflow did not have a significant impact on downwelling fluxes across the entire study reach ($p > 0.05$ for all comparisons of hydrologic cases; supporting information Table S2 and Figure S3).

In summary, groundwater inflow had a significant impact on the reach-scale hyporheic flow path residence time and length distributions during the spatially continuous stream discharge conditions (high and medium) and little to no impact during the spatially intermittent stream discharge condition (low). Downwelling flux did not have a significant response to groundwater inflow across the reach. The representation of groundwater inflow as spatially uniform or variable did have a significant impact on flow path residence time and length distributions, but only during high stream discharge.

3.2. Flow Path Responses to Different Stream Discharges and Groundwater Inflows

3.2.1. Stream Discharge as a Control

Hyporheic flow paths did not respond uniformly to changing stream discharge across the study reach. Flow path residence times both increased and decreased from the baseline cases in response to an increase in stream discharge (H-M; Figure 3a where each dot represents an individual flow path) and a decrease in stream discharge (L-M; Figure 3b). However, most changes from the M baseline were small (<5%; left histograms in Figure 3). The probability that the baseline flow path residence time would change in response to an increase in stream discharge was largest for residence times between 1 and 10 h, and similarly between 10 and 100 h (top histogram at order-of-magnitude intervals in Figure 3a). While a wide range of flow path

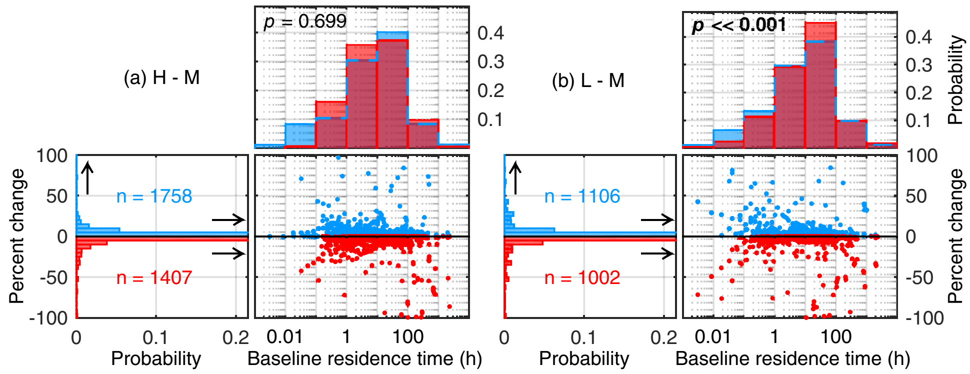

Figure 3. Stream discharge as a control on hyporheic flow path residence times, represented as increases (positive, blue) and decreases (negative, red) from the corresponding baseline residence times. (a) High (H) relative to medium (M) stream discharge with no groundwater inflow (see Table 1). (b) Low (L) stream discharge relative to M. The dot-plots provide all the percent changes as a function of the baseline flow path residence times. The left histograms are at 5% intervals. The top histograms are at order-of-magnitude intervals and represent the probability of which baseline flow path residence times will change due to an increase or decrease in stream discharge (overlap is designated by a dashed line). A *p* value < 0.05 indicates that the medians are statistically different (also indicated by bold text). Arrows designate values larger than displayed. See supporting information Figures S4 and S5 for changes in flow path lengths and fluxes.

residence times are sensitive to stream discharge, they fall toward the median of all possible residence times (Table 3 and Figure 2). A decrease in stream discharge resulted in a similar pattern regarding both increases and decreases in flow path residence time (Figure 3b). However, the distributions of baseline flow path residence times that increased and decreased in response to an increase in stream discharge were statistically the same ($p = 0.699$; top histogram in Figure 3a), suggesting that similar suites of flow path residence times are prone to both decreases and increases in response to increasing stream discharge. Conversely, the distributions of baseline flow path residence times that increased and decreased in response to a decrease in stream discharge were significantly different ($p \ll 0.001$; top histogram in Figure 3b).

Hyporheic flow path lengths also increased and decreased in response to stream discharge (supporting information Figure S4). The probability that the baseline flow path length would change in response to an increase or decrease in stream discharge was largest for lengths between 1 and 10 m (top histograms in supporting information Figure S4). This range falls on the lower side of possible lengths, where the maximum was ~300 m (supporting information Table S1 and Figure S2). Similar to residence time responses, the distributions of flow path lengths that increased or decreased were statistically the same in response to increasing stream discharge ($p = 0.762$; top histogram in supporting information Figure S4a), and significantly different in response to decreasing stream discharge ($p \ll 0.001$; top histogram in supporting information Figure S4b). Subsequently, the downwelling fluxes of the baseline flow paths both increased and decreased in response to changing stream discharge with the highest probability of downwelling fluxes that change between 0.1 and 1 m d^{-1} (supporting information Figure S5). This range falls on the lower side of possible fluxes, where the maximum was ~7 m d^{-1} (supporting information Table S2 and Figure S3).

Of the hyporheic flow paths with major changes (>5%), the shorter residence time flow paths tended to be more sensitive to an increase and decrease in stream discharge than the longer residence time flow paths (shown by the significantly different distributions in Figure 4). However, a large majority (~80%) of the flow paths persisted with only minor changes in residence time in response to changes in stream discharge. Consistently, the shorter length flow paths and smaller downwelling fluxes tended to be more sensitive to changing stream discharge (shown by the significantly different distributions in supporting information Figures S6 and S7). Although these results provide evidence that there are suites of flow paths more sensitive to stream discharge than others, there was substantial overlap in the distributions of baseline flow path residence times, lengths, and downwelling fluxes that increased, decreased, or persisted. This overlap further indicates that flow paths did not respond uniformly to changing stream discharge across the study reach.

3.2.2. Groundwater Inflow as a Control

In contrast to stream discharge as a control, hyporheic flow path residence times, lengths, and downwelling fluxes mostly decreased in response to groundwater inflow (Figure 5 and supporting information Figures

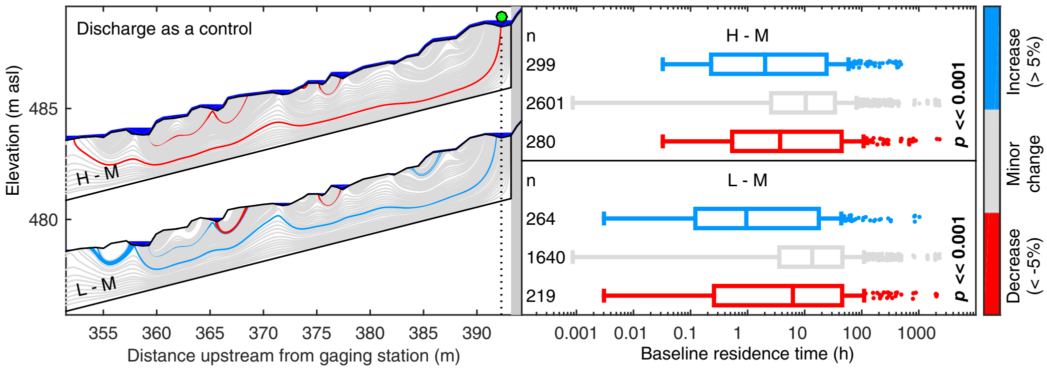

Figure 4. (left column; see Figure 2 for location) Example of the hyporheic flow paths with major changes in residence time in response to changing stream discharge. Flow paths in blue indicate increases >5%; flow paths in red indicate decreases >5% relative to the baseline. Here an increase (H) and decrease (L) in stream discharge is compared to the baseline of medium stream discharge with no groundwater inflow (M; see Table 1). (right column) The full reach distributions (box-and-whisker plots of the quantiles) of the baseline flow path residence times that have increased, decreased, or persisted (minor change < 5%). A p value < 0.05 indicates that the medians of at least one distribution are statistically different from another (also indicated by bold text). See supporting information Figures S6 and S7 for changes in flow path lengths and fluxes. See supporting information Figure S12 for a full reach view of the left column.

S8, and S9). The number of flow paths showing decreases was proportional to the amount of groundwater inflow—more flow paths decreased during high than during medium stream discharge while few flow paths were affected by groundwater inflow during low stream discharge. Similar to stream discharge as a control, there were both increases and decreases in flow path residence time and length in response to groundwater inflow (Figure 5 and supporting information Figure S8). The probability that a baseline flow path would decrease in residence time in response to groundwater inflow was largest for flow path residence times between 1 and 10 h, and between 10 and 100 h (top histograms in Figure 5). However, groundwater inflow caused a more pronounced separation between residence times that increased or decreased than did stream discharge as a control (shown by the significantly different distributions of baseline flow paths that increased or decreased in the top histograms of Figure 5), where more shorter residence time flow paths (<1 h) had a higher probability of increasing. The highest probability that flow path lengths would decrease in response to groundwater inflow was between 1 and 10 m (top histograms in supporting information Figure S8). Similar to the residence time response, there was a higher probability for flow paths shorter than 1 m to increase with increasing groundwater inflow. All the downwelling fluxes that changed decreased from the baseline, where the highest probability for change occurred between 0.1 and 1 m d^{-1} (supporting information Figure S9). This range again falls on the lower side of possible fluxes (supporting information Table S2 and Figure S3).

Of the hyporheic flow paths with major changes in residence times (>5%), the longer residence time flow paths tended to decrease while the shorter residence time flow paths tended to increase in response to groundwater inflow (shown by the significantly different distributions in Figures 6a–6c). The exceptions were that both the longer and shorter residence time flow paths tended to increase and decrease in response to uniform groundwater inflow during medium stream discharge (MU-M; Figure 6b) and in response to both representations of groundwater inflow during low stream discharge (LU-L and LV-L; Figure 6c). However, the flow paths that increased comprised only ~1% of all flow paths during medium stream discharge. During low stream discharge, only ~6% of all flow paths experienced major changes. The longer flow path lengths also tended to decrease in response to groundwater inflow (shown by the significantly different distributions in supporting information Figure S10). The smaller downwelling fluxes tended to be more sensitive to groundwater inflow (shown by the significantly different distributions in supporting information Figure S11). Flow paths longer in residence time and length, or those with smaller downwelling fluxes, tended to be more sensitive to groundwater inflow than those with shorter residence times and lengths, or larger downwelling fluxes. While the flow paths more consistently decreased in response to groundwater inflow than in response to stream discharge, there was again substantial overlap in the distributions of flow paths that increased, decreased, or persisted.

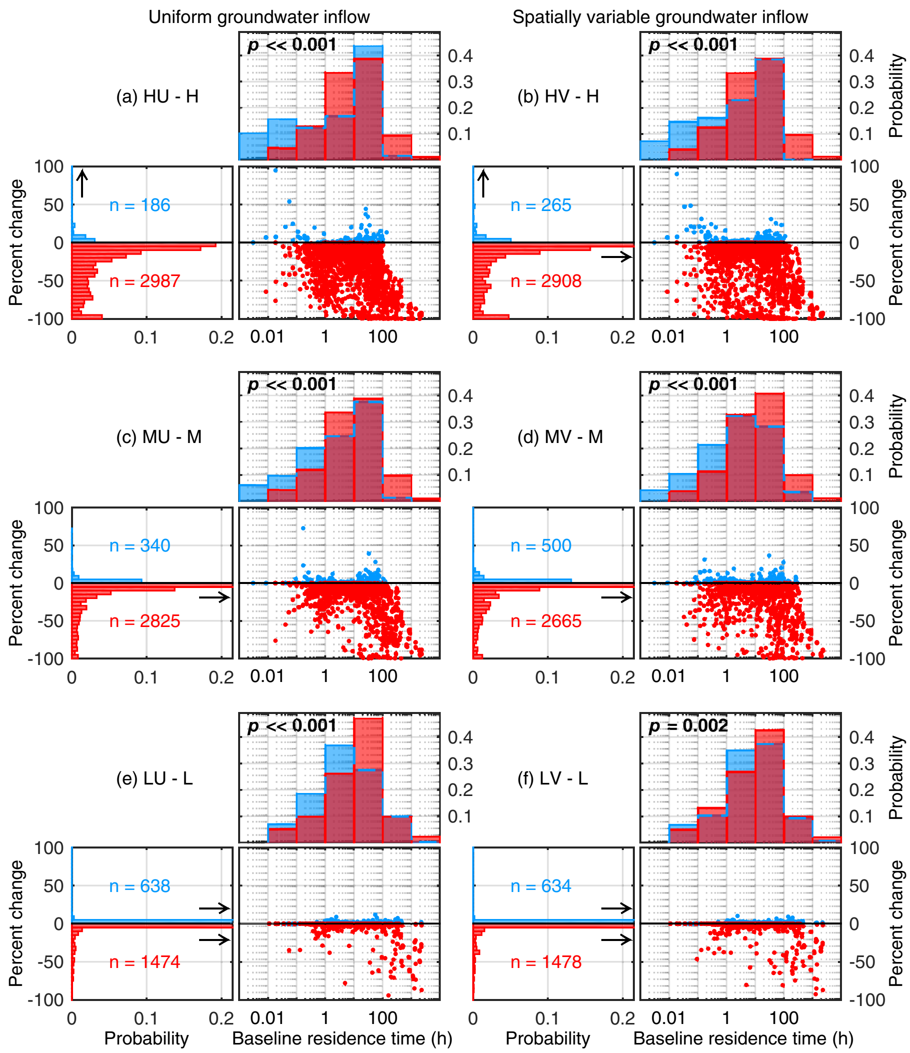

Figure 5. Groundwater inflow (left column uniform, right column spatially variable) as a control on hyporheic flow path residence times, represented as increases (blue, positive) and decreases (negative, red) from the baseline hydrologic cases of high (H), medium (M), and (L) stream discharge with no groundwater inflow (see Table 1). (a) Uniform (HU) and (b) spatially variable (HV) groundwater inflow relative to H. (c) Uniform (MU) and (d) spatially variable (MV) groundwater inflow relative to M. (e) Uniform (LU) and (f) spatially variable (LV) groundwater inflow relative to L. The dot-plots provide all the changes as a function of the associated baseline flow path residence time. The left histograms are at 5% intervals. The top histograms are at order-of-magnitude intervals and represent the probability of which baseline flow path residence times will respond to changing groundwater inflow (overlap is designated by a dashed line). A p value < 0.05 indicates the medians are statistically different (also indicated by bold text). Arrows indicate values larger than displayed. See supporting information Figures S8 and S9 for changes in flow path lengths and fluxes.

4. Discussion

4.1. Expected Hydrologic Controls in Confined Mountainous Stream Corridors

We built a heuristic model to represent the dominant hydrologic controls on hyporheic exchange in mountainous stream corridors constrained by bedrock, confined by steep hillslopes, and with step-pool morphology. We assumed that the dominant hydrologic controls would be changes to the hydrostatic water surface profile and groundwater inflow under different stream discharge and catchment wetness conditions. We ignored influences from hydrodynamic contributions, planform morphology such as sinuosity and side-channels, and lateral inputs based on previous work in similar settings [e.g., *Gooseff et al.*, 2006; *Kasahara and Wondzell*, 2003]. Although our model is heuristic and not meant to provide a calibrated, site-specific representation, it is based on observations, represents realistic arrangements of streambed morphologic features, and examines how different hydrologic conditions control hyporheic flow paths in mountainous settings. In such settings, the down-valley hydraulic gradient is expected to remain relatively static over

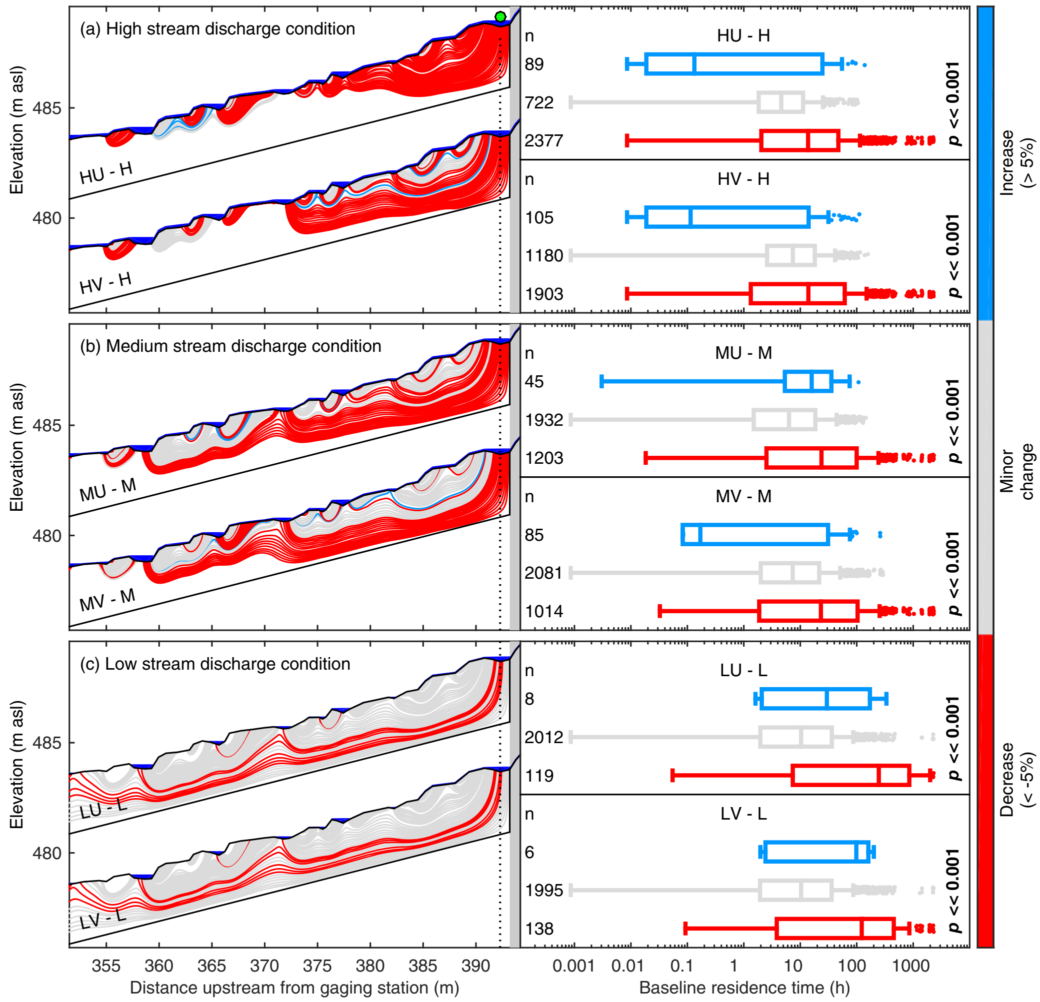

Figure 6. (left column; see Figure 2 for location) Example of the hyporheic flow paths with major changes in residence time in response to uniform or spatially variable groundwater inflow (U and H) relative to the (a) high, (b) medium, and (c) low stream discharge with no groundwater inflow baseline cases (H, M, and L; see Table 1). Flow paths in blue indicate increases >5%; flow paths in red indicate decreases >5% relative to the baseline. (right column) The full reach distributions (box-and-whisker plots of the quantiles) of the baseline flow path residence times that have increased, decreased, or persisted (minor change < 5%). A *p* value < 0.05 indicates the medians of at least one distribution are statistically different from another (also indicated by bold text). See supporting information Figures S10 and S11 for flow path lengths and fluxes.

different stream discharge conditions [*Voltz et al.*, 2013]. Therefore, we should expect that the shape of the water surface profile would be preserved across a wide range of stream discharges and thus have little influence on hyporheic flow paths. Our model results confirmed this expectation (Figure 2), showing that hyporheic exchange along the thalweg in mountain stream corridors is unlikely to be sensitive to changes in stream stage. Furthermore, because the range of stream discharges that we examined spans 95.6% (0.6 L s^{-1}) to 38.4% (25.0 L s^{-1}) exceedance probabilities, we expect that our results will be robust for over half of the year. It is possible that, at much higher stream discharges, channel morphologic features would be drowned out, wetted channel areas increase, and side channels activate, and thus have a large effect on lateral hyporheic exchange [*Ward et al.*, 2016; *Wondzell and Gooseff*, 2013]. However, these effects were likely not dominant over the range of discharges we examined as there was no visual activation of side channels.

Although we use observations to approximate a realistic water surface profile for each stream discharge, curvature in the profile due to rapidly varied flow—potentially not captured well in the observations (e.g., hydraulic jumps around step features)—can force hyporheic flow paths in the upstream direction [*Endreny et al.*, 2011]. While consideration of hydraulic jumps across different stream discharges may be important in mountainous stream corridors, we do not anticipate that omitting corresponding flow paths would significantly change our results due to the large number of flow paths already considered and anticipated dominance of hydrostatic drivers of exchange in this geomorphic setting [*Wondzell and Gooseff*, 2013].

Hyporheic exchange can be quite different in lower-gradient streams where hydrodynamic processes are often dominant and, because stream velocity increases with discharge, is expected to be more sensitive to changing stream discharge [e.g., *Wondzell and Gooseff*, 2013]. Of course, channel morphologic features like riffles can also be drowned out at high discharge in low-gradient river corridors and reduce the extent of hyporheic exchange [*Storey et al*., 2003]. Subsequently, there can be relatively steeper lateral gradients between the channel and floodplain due to a less dominant down-valley gradient. In such cases, groundwater inflow can have a minor impact on hyporheic exchange [*Storey et al*., 2003]. Groundwater inflow is more likely to be a primary control in mountainous settings [*Caruso et al*., 2016], which is consistent with our findings (Figure 5). Overall, the modeling approach we used allowed us to effectively examine hydrologic controls in this mountain stream.

4.2. Evidence of Suites of Flow Paths Sensitive to Different Hydrologic Conditions

Our results showed that some suites of flow paths are more prone to change than others in response to changes in stream discharge and groundwater inflow. In general, we found that, with our two-dimensional model of a confined mountain stream corridor, hyporheic exchange was more sensitive to changing groundwater inflow than to changing stream discharge. Specifically, most hyporheic flow paths did not change as discharge changed by over an order-of-magnitude. Only about 10–20% of the flow paths showed changes greater than 5% in residence times, lengths, and fluxes over the range of stream discharges examined (Figure 4 and supporting information Figures S6 and S7). These results clearly indicate that stream discharge is not a primary control on hyporheic exchange relative to morphologic controls, because most flow paths induced by the channel morphology were persistent in the face of changing discharge. While only a relatively small number of flow paths changed, our simulations suggest that shorter residence time flow paths tended to both increase (median 1–2 h) and decrease (median 3–5 h) in response to changing stream discharge (Figure 4). Although it may appear counter-intuitive, this pattern held true for both increases and decreases in discharge relative to the medium baseline case (shown by the significantly different distributions in Figure 4). Remember, however, that the stream became spatially intermittent during low stream discharge whereas it was contiguously wetted during both the medium and high stream discharges. Similarly, the shorter length flow paths tended to both increase (median $\sim$0.1 m) and decrease (median $\sim$0.2 m) in response to stream discharge (supporting information Figure S6), and flow paths associated with the smallest downwelling fluxes (median $\sim$0.15 m d^{-1}) tended to be more sensitive to changing stream discharge conditions (supporting information Figure S7).

The influence of groundwater depended greatly on the magnitude of inflows. Under high stream discharge, groundwater inflows were large and substantially truncated hyporheic flow paths, with more than 70% showing major decreased residence times, lengths, and downwelling fluxes under uniformly distributed inflows (Figures 6 and supporting information S10 and S11). Only approximately 20% of the flow paths persisted (change $<$5% relative to the no groundwater inflow baseline case). If inflows during high stream discharge were distributed according to UAA, however, approximately 40% of the flow paths persisted and roughly 60% decreased (very few increased). These results are broadly consistent with the literature showing potentially large impacts of groundwater inflows on hyporheic exchange [e.g., *Gomez-Velez et al*., 2015; *Cardenas and Wilson*, 2007a; *Boano at al*., 2008]. More importantly, the catchment topology may significantly influence the location, length, residence time, and amount of hyporheic exchange along the stream network, preferentially collapsing the hyporheic zone where large UAA connects to the valley bottom [*Caruso et al*., 2016]. Our results confirm that catchment topology is an important influence on hyporheic flow paths, but is only significant during high stream discharge (Table 2).

Groundwater inflows were much smaller during the medium and low stream discharge and thus their influence on the hyporheic zone was smaller. Some 60–70% of the flow paths persisted under medium stream discharge and more than 90% persisted under low stream discharge with little difference between the uniform and spatially variable inflow cases (Figure 6 and supporting information Figures S10 and S11). In all groundwater inflow cases, however, the flow paths with longer residence times (medians $>$ 10 h) tended to decrease and, while flow paths whose residence times increased were uncommon ($<$ 3% in all cases), these tended to be of much shorter duration (Figure 6). Likewise, the longer length flow paths (medians $>$ 2 m) tended to decrease (supporting information Figure S10) as did those with smaller downwelling fluxes (supporting information Figure S11).

If the only source of water to the subsurface is stream water, as in our no-groundwater inflow simulations, the numerical model will necessarily simulate hyporheic flow paths of sufficient length and duration to saturate subsurface flows throughout the model domain. Consequently, some hyporheic flow paths could be artificially made long by depth of sediment and considered an artifact of the modeling structure. However, we have explicitly tested the persistence of such flow paths under representative conditions. Our results, showing that very long flow paths are present in the medium and low stream discharge cases, suggest that these flow paths are realistic and not simply an artifact of our model structure. Furthermore, our model results are broadly consistent with a number of tracer studies conducted in a densely instrumented well network that demonstrate persistent, long-residence time flow paths over a wide range of stream discharges [e.g., *Ward et al.*, 2016; *Wondzell*, 2006]. Our model shows that these longer flow paths remain in the lower part of the colluvium stored in the valley, with fluxes driven by the valley gradient (~12%), generating long residence times (up to 96 days in our model), but accounting for relatively little of the total hyporheic flux within the reach. These long flow paths are readily truncated by groundwater inflows if the magnitude of those inflows is sufficient to displace a large amount of the hyporheic water. However, the groundwater inflows are, themselves, captured in these long, down-valley flow paths and, because of the nested structure of the flow paths, only enter the stream in locations where channel morphologic features generate upwelling zones. Thus, shorter residence time and length flow paths persist. These persistent flow paths are likely generated by steep local gradients around steps in the longitudinal profile of the stream surface, and consequently have relatively high flux and short length and residence times.

4.3. Hyporheic Flow Paths Do Not Respond Uniformly to Stream Discharge or Groundwater Inflow

There were some locations where flow paths persisted in the face of both changing stream discharge and groundwater inflow (callout (1) in Figure 7a), locations where flow paths were sensitive to groundwater inflow but not to stream discharge (callout (2) in Figure 7a), and locations where flow paths were sensitive to stream discharge but not to groundwater inflow (callout (3) in Figure 7a). We propose that the sensitivity of flow paths to hydrologic controls is a function of the local hydraulic gradient mainly set by the streambed morphology. Flow paths that occurred with larger hydraulic gradients, such as those created by large features like a step-pool sequence, were the most persistent (Figures 7b and 7c). Flow paths that occurred with hydraulic gradients similar to the valley gradient—which tended to be longer in length and residence time—were generally the most sensitive to changes in hydrologic conditions. The exception is at locations where groundwater inflow may not be focused (HV-H callout (3) in Figure 7a). This relationship explains why *Ward et al.* [2016] found that hyporheic flow paths near the stream did not change in response to changing stream discharge—the hydraulic gradients set by the streambed morphology were dominant. Nonuniform responses to flow paths could complicate the upscaling of feature-scale knowledge to make

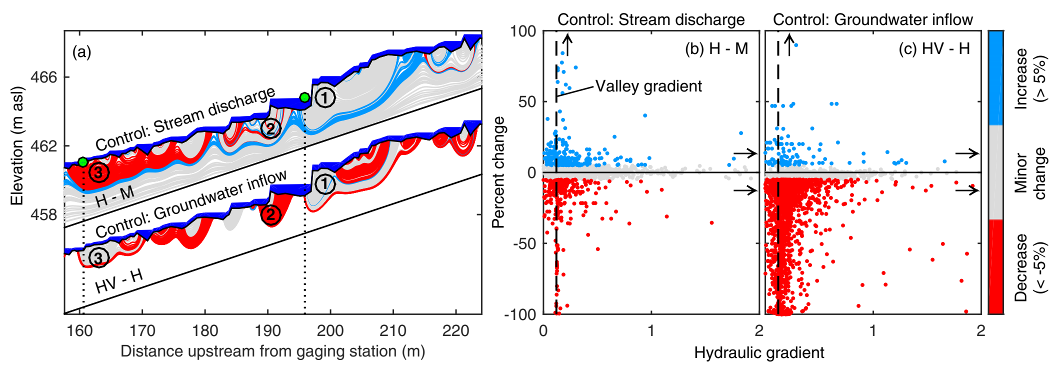

Figure 7. (a) Example of the hyporheic flow paths with major changes in residence time in response to an increase in stream discharge from medium to high (M and H) and spatially variable groundwater inflow during high stream discharge (HV; Table 1; see Figure 2 for location). Flow paths in blue indicate increases >5%; flow paths in red indicate decreases >5% relative to the baseline. Callouts in panel (a) indicate locations where flow paths are (1) not sensitive to changing discharge or groundwater inflow, (2) sensitive to groundwater inflow but not discharge, and (3) sensitive to discharge but not groundwater inflow. All percent changes in response to changing (b) stream discharge and (c) groundwater inflow as a function of the hydraulic gradient along the hyporheic flow path. This gradient is approximated from the downwelling (starting) and upwelling (ending) location of each flow path. Arrows indicate values larger than displayed.

predictions at larger network scales. When groundwater inflow is high enough to overwhelm the hydraulic gradient set by streambed morphology, most of the flow paths are reduced in residence time, length, and downwelling flux—only flow paths driven by the largest changes in morphology persist. We recommend that refined relationships include consideration of hydraulic gradients set by morphology to better represent locations and suites of flow paths that are more sensitive to hydrologic controls.

We also recognize that unsteady hydrologic conditions may be important when predicting hyporheic flow path distributions and response [e.g., *Dudley-Southern and Binley*, 2015; *Schmadel et al*., 2016; *Ward et al*., 2014, 2016; *Zimmer and Lautz*, 2014]. Steady simulations have shown that vertical exchange is typically set by morphology [*Gomez-Velez et al*., 2015; *Precht and Huettel*, 2003; *Sawyer et al*., 2013] and groundwater inflow typically reduces the role of morphologically driven exchange [e.g., *Boano et al*., 2007; *Cardenas and Wilson*, 2007a; *Fox et al*., 2014]. Although our steady simulations indicate that the arrangement of morphologic features may cause nonuniform responses to changes in stream discharge, they indicate that stream discharge is a secondary control relative to morphologically driven hyporheic exchange. Because we found that the longest flow paths and those that originated from the smallest downwelling fluxes were the most sensitive to groundwater inflow, long flow paths that persist during low discharge conditions may be forced back to the stream when discharge (and corresponding groundwater inflow) increases. Likewise, an unsteady decrease in stream discharge may cause flow path lengths and residence times to increase. The next steps toward a comprehensive understanding of hydrologic controls on hyporheic exchange, and ultimately aggregate feature-scale responses to larger network scales, will need to incorporate dynamic hydrologic changes across different valley settings.

The perspective of how hyporheic flow paths respond to different hydrologic conditions depends on the spatial scale of observations. We found that, at the reach scale, groundwater inflow generally reduced flow path residence time and length, and reduced associated downwelling flux, during periods of spatially continuous stream discharge. At this scale, spatially continuous stream discharge alone did not significantly influence hyporheic flow paths. These results suggest that there is a systematic response in hyporheic exchange across different hydrologic conditions at the reach scale, such that groundwater inflow reduces flux and flow path residence time and length only during periods of spatial continuity by primarily acting on the longest flow paths; in contrast, shorter flow paths driven by morphology persist across different hydrologic conditions. However, individual flow paths did not respond uniformly due to the heterogeneous arrangement of morphologic features. Similar results have been seen in other studies conducted under different hydrologic and geomorphic conditions [e.g., *Dudley-Southern and Binley*, 2015; *Zimmer and Lautz*, 2014]. The scale-dependency of hyporheic responses suggests that care must be taken when aggregating the influence of individual morphologic features to represent an entire stream reach or large stream network because, in mountain stream networks, their influence can change substantially as groundwater inflows also change. A number of authors have aggregated the influence of feature-scale processes to very large stream networks, albeit, in low-gradient stream networks [*Gomez-Velez et al*., 2015; *Kiel and Cardenas*, 2014]. These studies have, to date, only examined the relative influence of hydrodynamic exchange from stream bed forms and hydrostatic exchange across meander bends created by sinuous stream channels. Other factors driving (or limiting) hyporheic exchange within these large river networks have mostly not been examined, suggesting that further work considering a fuller suite of processes and their dynamics might prove useful to better understand the role of the hyporheic zone at large scales.

4.4. Time Scales, Flux Magnitudes, and the Importance of Hyporheic Exchange to Stream and Watershed Ecosystem Processes

The influence of surface water-groundwater interactions on downstream water quality is an emergent property resulting from aggregation of the suite of processes that occur along reasonably long reaches of a stream or large portions of a stream network. The specific influence "emerges" from the amount and residence time of stream water in the subsurface, the arrangement of these subsurface exchanges in space, and how, together, these factors relate to the timescales of processes of interest. Empirically based studies are needed to help inform representation of these processes; however, many (perhaps most) previous studies examining the role of morphologic features as drivers of hyporheic exchange have been beset by problems with the "spatial windows of detection" that have most typically biased those studies to examine relatively short flow paths [e.g., *Cardenas and Wilson*, 2007b]. Similarly for the temporal window of detection, if using a field tool (e.g., solute tracers) to interpret hyporheic flow path residence times at the reach scale, only the fastest fraction of flow paths will be observed ("short-term storage" after *Ward et al*.[2013b]). Studies with observation well networks have demonstrated that substantial hyporheic exchange can occur at spatial and temporal scales much larger than the windows of detection in typical stream tracer-based studies [e.g., *Harvey et al*., 1996; *Triska et al*., 1993; *Ward et al*., 2016; *Wondzell et al*., 2009]. Thus, a large portion of hyporheic flow paths remain essentially unstudied ("long-term storage" after *Ward et al*.[2013b]). However, the representation of hyporheic flow paths depends on the objectives of the study. For example, if denitrification is the process of interest, flow paths with residence times between 7 and 30 h are of critical concern [e.g., *Marzadri et al*., 2014; *Zarnetske et al*., 2011]. In the mountain stream corridor that we simulated, these are the flow paths most sensitive to groundwater inflows, indicating that a process like denitrification could be regulated by hydrologic controls rather than by morphology. Similarly, the ability to predict the legacy of pollutants requires an accurate representation of very long residence time flow paths. Our simulations suggest that turnover of hyporheic water on long flow paths could be driven by increased groundwater inflows during a storm, as has been observed elsewhere [*Godsey and Kirchner*, 2014; *Jencso et al*., 2010, 2009] and potentially push substantial amounts of polluted water into the stream, long after the surface pulse is no longer measurable. Our simulations suggest that turnover of hyporheic water is not a uniform, bulk process, but rather results from suites of flow paths with different sensitivities to hydrologic controls. If our understanding of these exchange processes is based on studies with limited spatial and temporal windows of detection, the critical flow paths that dictate pollutant legacy could be completely overlooked.

5. Conclusions

We used a two-dimensional, profile model of a 600 m study reach to examine how stream discharge and groundwater inflow control reach-scale hyporheic exchange in confined mountainous stream corridors with observed step-pool morphology. We showed that changing stream discharge had little influence on hyporheic exchange, even across a wide range of stream discharges. Rather, exchange flows were driven almost exclusively by streambed morphology, where the effective morphology of our simulations did not change over the range of stream discharges we examined. We also showed that the influence of groundwater inflows depended greatly on their magnitude. However, groundwater inflows did not influence all hyporheic exchange flows equally. When groundwater inflows were large, they had their greatest influence on the longest hyporheic flow paths—flow paths with long residence times, lengths, and relatively small exchange fluxes. We also found some evidence that, when groundwater inflows were high, catchment topology represented by differences in upslope accumulated area draining into the stream corridor could influence the location and persistence of hyporheic flow paths. Finally, under drier conditions, when the stream was spatially intermittent, groundwater inflows were far too small to noticeably influence hyporheic flow paths. Overall, we conclude that flow paths originating where large changes in channel morphology create steep hydraulic gradients are the least sensitive to changes in hydrologic conditions. Conversely, flow paths occurring with hydraulic gradients similar to the mean valley gradient are the most sensitive to changing hydrologic conditions. Because groundwater inflows are a function of catchment wetness, which itself is a function of seasonal-scale and storm-scale weather drivers, we can anticipate which suites of flow paths are more likely to respond to changes in hydrologic controls. Ultimately, we recommend that relationships between hydrologic and morphologic controls be refined to more accurately differentiate between hyporheic flow paths that persist in time and those that are sensitive to changing hydrologic conditions. Only then will we be able to aggregate feature-scale knowledge to more accurately infer transport at the network scale in mountainous catchments.

Acknowledgments
Tools for spatial data processing were developed by Ward and Schmadel with support provided in part by NSF grants EAR 1505309 and EAR 1331906. Ward was also supported by NSF grant EAR 1652293, the Indiana University Office of the Vice Provost for Research and the Indiana Water Resources Research Center. Wondzell was supported by NSF grant EAR 1417603. Field campaigns were funded in part by the Leverhulme International Network's "Where rivers, groundwater and disciplines meet: a hyporheic research network." The authors thank Jase Hixson, Kerry Neil, Stephen Plont, and Brynn O'Donnell for help with data collection. Facilities and additional data were provided by the H. J. Andrews Experimental Forest research program, funded by the NSF's Long-Term Ecological Research Program (DEB-1440409), U.S. Forest Service Pacific Northwest Research Station, and Oregon State University. Any opinions, findings, and conclusions or recommendations expressed in this material are those of the authors and do not necessarily reflect the views of the National Science Foundation, U.S. Forest Service, H. J. Andrews Experimental Forest, Oregon State University, or Indiana University. Precipitation, discharge, and spatial data are available from H. J. Andrews Experimental Forest Data Catalog (http://andrewsforest.oregonstate.edu/). The research was conceptualized and written by N. M. S., A. S. W., and S. M. W. N. M. S. led the numerical modeling and data analysis tasks. Topographic survey data, water level data, and simulation results are available upon request to the corresponding author. The authors report no conflicts of interest. We thank the editors and three anonymous reviewers for their thoughtful comments to help improve this manuscript.

References

Amatya, D. M., J. Campbell, P. Wohlgemuth, K. Elder, S. Sebestyen, S. Johnson, E. Keppeler, M. B. Adams, P. Caldwell, and D. Misra (2016), Hydrological processes of reference watersheds in Experimental Forests, USA, in *Forest Hydrology: Processes, Management, and Applications*, edited by D. Amatya et al., pp. 219–239, CABI Publ., U. K.

Boano, F., R. Revelli, and L. Ridolfi (2007), Bedform-induced hyporheic exchange with unsteady flows, *Adv. Water Resour.*, *30*(1), 148–156.

Boano, F., R. Revelli, and L. Ridolfi (2008), Reduction of the hyporheic zone volume due to the stream-aquifer interaction, *Geophys. Res. Lett.*, *35*, L09401, doi:10.1029/2008GL033554.

Boano, F., R. Revelli, and L. Ridolfi (2013), Modeling hyporheic exchange with unsteady stream discharge and bedform dynamics, *Water Resour. Res.*, *49*, 4089–4099, doi:10.1002/wrcr.20322.

Boano, F., J. W. Harvey, A. Marion, A. I. Packman, R. Revelli, L. Ridolfi, and A. Wörman (2014), Hyporheic flow and transport processes: Mechanisms, models, and biogeochemical implications, *Rev. Geophys.*, *52*, 603–679, doi:10.1002/2012RG000417.

Botros, F. E., T. Harter, Y. S. Onsoy, A. Tuli, and J. W. Hopmans (2009), Spatial Variability of Hydraulic Properties and Sediment Characteristics in a Deep Alluvial Unsaturated Zone All rights reserved. No part of this periodical may be reproduced or transmitted in any form or by any means, electronic or mechanical, including photocopying, recording, or any information storage and retrieval system, without permission in writing from the publisher, *Vadose Zone J.*, *8*(2), 276–289.

Buffington, J. M., and D. Tonina (2009), Hyporheic exchange in mountain rivers. II: Effects of channel morphology on mechanics, scales, and rates of exchange, *Geogr. Compass*, *3*(3), 1038–1062.

Cardenas, M. B., and J. L. Wilson (2007a), Exchange across a sediment-water interface with ambient groundwater discharge, *J. Hydrol.*, *346*(3–4), 69–80.

Cardenas, M. B., and J. L. Wilson (2007b), Hydrodynamics of coupled flow above and below a sediment-water interface with triangular bedforms, *Adv. Water Resour.*, *30*(3), 301–313.

Carey, G. R., E. A. McBean, and S. Feenstra (2016), Estimating tortuosity coefficients based on hydraulic conductivity, *Ground Water*, *54*(4), 476–487.

Caruso, A., L. Ridolfi, and F. Boano (2016), Impact of watershed topography on hyporheic exchange, *Adv. Water Resour.*, *94*, 400–411.

Castro, N. M., and G. M. Hornberger (1991), Surface-subsurface water interactions in an alluviated mountain stream channel, *Water Resour. Res.*, *27*(7), 1613–1621.

Church, M., and A. Zimmermann (2007), Form and stability of step-pool channels: Research progress, *Water Resour. Res.*, *43*, W03415, doi:10.1029/2006WR005037.

Corson-Rikert, H. A., S. M. Wondzell, R. Haggerty, and M. V. Santelmann (2016), Carbon dynamics in the hyporheic zone of a headwater mountain stream in the Cascade Mountains, Oregon, *Water Resour. Res.*, *52*, 7556–7576, doi:10.1002/2016WR019303.

Downer, C. W., and F. L. Ogden (2004), Appropriate vertical discretization of Richards' equation for two-dimensional watershed-scale modelling, *Hydrol. Processes*, *18*(1), 1–22.

Dudley-Southern, M., and A. Binley (2015), Temporal responses of groundwater-surface water exchange to successive storm events, *Water Resour. Res.*, *51*, 1112–1126, doi:10.1002/2014WR016623.

Dunne, T., and L. B. Leopold (1978), *Water in Environmental Planning*, edited by W. H. Freeman, New York.

El-Kadi, A. I. (2005), Validity of the generalized Richards equation for the analysis of pumping test data for a coarse-material aquifer, *Vadose Zone J.*, *4*(1), 196–205.

Endreny, T., L. Lautz, and D. I. Siegel (2011), Hyporheic flow path response to hydraulic jumps at river steps: Flume and hydrodynamic models, *Water Resour. Res.*, *47*, W02517, doi:10.1029/2009WR008631.

Fox, A., F. Boano, and S. Arnon (2014), Impact of losing and gaining streamflow conditions on hyporheic exchange fluxes induced by dune-shaped bed forms, *Water Resour. Res.*, *50*, 1895–1907, doi:10.1002/2013WR014668.

Francis, B. A., L. K. Francis, and M. B. Cardenas (2010), Water table dynamics and groundwater-surface water interaction during filling and draining of a large fluvial island due to dam-induced river stage fluctuations, *Water Resour. Res.*, *46*, W07513, doi:10.1029/2009WR008694.

Gerecht, K. E., M. B. Cardenas, A. J. Guswa, A. H. Sawyer, J. D. Nowinski, and T. E. Swanson (2011), Dynamics of hyporheic flow and heat transport across a bed-to-bank continuum in a large regulated river, *Water Resour. Res.*, *47*, W03524, doi:10.1029/2010WR009794.

Godsey, S. E., and J. W. Kirchner (2014), Dynamic, discontinuous stream networks: Hydrologically driven variations in active drainage density, flowing channels and stream order, *Hydrol. Processes*, *28*(23), 5791–5803.

Gomez-Velez, J. D., and J. W. Harvey (2014), A hydrogeomorphic river network model predicts where and why hyporheic exchange is important in large basins, *Geophys. Res. Lett.*, *41*, 6403–6412, doi:10.1002/2014GL061099.

Gomez-Velez, J. D., J. W. Harvey, M. B. Cardenas, and B. Kiel (2015), Denitrification in the Mississippi River network controlled by flow through river bedforms, *Nat. Geosci.*, *8*(12), 941–945.

Gooseff, M. N., J. K. Anderson, S. M. Wondzell, J. LaNier, and R. Haggerty (2006), A modelling study of hyporheic exchange pattern and the sequence, size, and spacing of stream bedforms in mountain stream networks, Oregon, USA, *Hydrol. Processes*, *20*(11), 2443–2457.

Harvey, J., and M. Gooseff (2015), River corridor science: Hydrologic exchange and ecological consequences from bedforms to basins, *Water Resour. Res.*, *51*, 6893–6922, doi:10.1002/2015WR017617.

Harvey, J. W., B. J. Wagner, and K. E. Bencala (1996), Evaluating the reliability of the stream tracer approach to characterize stream-subsurface water exchange, *Water Resour. Res.*, *32*(8), 2441–2451.

Hassan, M. A., D. Tonina, R. D. Beckie, and M. Kinnear (2015), The effects of discharge and slope on hyporheic flow in step-pool morphologies, *Hydrol. Processes*, *29*(3), 419–433.

Irvine, D. J., and L. K. Lautz (2015), High resolution mapping of hyporheic fluxes using streambed temperatures: Recommendations and limitations, *J. Hydrol.*, *524*, 137–146.

Jackman, A. P., R. A. Walters, and V. C. Kennedy (1984), Transport and concentration controls for chloride, strontium, potassium and lead in Uvas Creek, a small cobble-bed stream in Santa Clara County, California, U.S.A, *J. Hydrol.*, *75*(1), 111–141.

Jencso, K. G., B. L. McGlynn, M. N. Gooseff, S. M. Wondzell, K. E. Bencala, and L. A. Marshall (2009), Hydrologic connectivity between landscapes and streams: Transferring reach- and plot-scale understanding to the catchment scale, *Water Resour. Res.*, *45*, W04428, doi:10.1029/2008WR007225.

Jencso, K. G., B. L. McGlynn, M. N. Gooseff, K. E. Bencala, and S. M. Wondzell (2010), Hillslope hydrologic connectivity controls riparian groundwater turnover: Implications of catchment structure for riparian buffering and stream water sources, *Water Resour. Res.*, *46*, W10524, doi:10.1029/2009WR008818.

Kasahara, T., and S. M. Wondzell (2003), Geomorphic controls on hyporheic exchange flow in mountain streams, *Water Resour. Res.*, *39*(1), 1005, doi:10.1029/2002WR001386.

Kiel, B. A., and M. B. Cardenas (2014), Lateral hyporheic exchange throughout the Mississippi River network, *Nat. Geosci.*, *7*(6), 413–417.

Malzone, J. M., C. S. Lowry, and A. S. Ward (2016), Response of the hyporheic zone to transient groundwater fluctuations on the annual and storm event time scales, *Water Resour. Res.*, *52*, 5301–5321, doi:10.1002/2015WR018056.

Marzadri, A., D. Tonina, A. Bellin, and J. L. Tank (2014), A hydrologic model demonstrates nitrous oxide emissions depend on streambed morphology, *Geophys. Res. Lett.*, *41*, 5484–5491, doi:10.1002/2014GL060732.

Mualem, Y. (1976), A new model for predicting the hydraulic conductivity of unsaturated porous media, *Water Resour. Res.*, *12*(3), 513–522.

Niswonger, R., and D. Prudic (2004), Modeling variably saturated flow using kinematic waves in MODFLOW, in *Groundwater Recharge in a Desert Environment, Water Sci. Appl.*, pp. 101–112, edited by J. F. Hogan, F. M. Phillips, and B. R. Scanlon, AGU, Washington, D. C.

Packman, A. I., M. Salehin, and M. Zaramella (2004), Hyporheic exchange with gravel beds: Basic hydrodynamic interactions and bedform-induced advective flows, *J. Hydraul. Eng.*, *130*(7), 647–656.

Precht, E., and M. Huettel (2003), Advective pore-water exchange driven by surface gravity waves and its ecological implications, *Limnol. Oceanogr.*, *48*(4), 1674–1684.

Richards, L. A. (1931), Capillary conduction of liquids through porous mediums, *J. Appl. Phys.*, *1*(5), 318–333.

Sawyer, A. H., M. Bayani Cardenas, A. Bomar, and M. Mackey (2009), Impact of dam operations on hyporheic exchange in the riparian zone of a regulated river, *Hydrol. Processes*, *23*(15), 2129–2137.

Sawyer, A. H., F. Shi, J. T. Kirby, and H. A. Michael (2013), Dynamic response of surface water-groundwater exchange to currents, tides, and waves in a shallow estuary, *J. Geophys. Res. Oceans*, *118*, 1749–1758, doi:10.1002/jgrc.20154.

Schmadel, N. M., A. S. Ward, C. S. Lowry, and J. M. Malzone (2016), Hyporheic exchange controlled by dynamic hydrologic boundary conditions, *Geophys. Res. Lett.*, *43*, 4408–4417, doi:10.1002/2016GL068286.

Schwanghart, W., and N. J. Kuhn (2010), TopoToolbox: A set of Matlab functions for topographic analysis, *Environ. Modell. Software*, *25*(6), 770–781.

Seibert, J., and B. L. McGlynn (2007), A new triangular multiple flow direction algorithm for computing upslope areas from gridded digital elevation models, *Water Resour. Res.*, *43*, W04501, doi:10.1029/2006WR005128.

Spies, T. (2016), *LiDAR Data (August 2008) for the Andrews Experimental Forest and Willamette National Forest Study Areas*, Long-term Ecol. Res., For. Sci. Data Bank, Corvalliss, Oreg. [Database]. [Available at http://andrewsforest.oregonstate.edu/data/abstract.cfm?dbcode=GI010, 18 Aug. 2016.]

Stonedahl, S. H., J. W. Harvey, A. Wörman, M. Salehin, and A. I. Packman (2010), A multiscale model for integrating hyporheic exchange from ripples to meanders, *Water Resour. Res.*, *46*, W12539, doi:10.1029/2009WR008865.

Stonedahl, S. H., J. W. Harvey, and A. I. Packman (2013), Interactions between hyporheic flow produced by stream meanders, bars, and dunes, *Water Resour. Res.*, *49*, 5450–5461, doi:10.1002/wrcr.20400.

Storey, R. G., K. W. F. Howard, and D. D. Williams (2003), Factors controlling riffle-scale hyporheic exchange flows and their seasonal changes in a gaining stream: A three-dimensional groundwater flow model, *Water Resour. Res.*, *39*(2), 1034, doi:10.1029/2002WR001367.

Tarboton, D. G. (1997), A new method for the determination of flow directions and upslope areas in grid digital elevation models, *Water Resour. Res.*, *33*(2), 309–319.

Tonina, D., and J. M. Buffington (2009), Hyporheic exchange in mountain rivers. I: Mechanics and environmental effects, *Geogr. Compass*, *3*(3), 1063–1086.

Tonina, D., and J. M. Buffington (2011), Effects of stream discharge, alluvial depth and bar amplitude on hyporheic flow in pool-riffle channels, *Water Resour. Res.*, *47*, W08508, doi:10.1029/2010WR009140.

Trauth, N., C. Schmidt, U. Maier, M. Vieweg, and J. H. Fleckenstein (2013), Coupled 3-D stream flow and hyporheic flow model under varying stream and ambient groundwater flow conditions in a pool-riffle system, *Water Resour. Res.*, *49*, 5834–5850, doi:10.1002/wrcr.20442.

Trauth, N., C. Schmidt, M. Vieweg, S. E. Oswald, and J. H. Fleckenstein (2015), Hydraulic controls of in-stream gravel bar hyporheic exchange and reactions, *Water Resour. Res.*, *51*, 2243–2263, doi:10.1002/2014WR015857.

Triska, F. J., J. H. Duff, and R. J. Avanzino (1993), Patterns of hydrological exchange and nutrient transformation in the hyporheic zone of a gravel-bottom stream: Examining terrestrial—Aquatic linkages, *Freshwater Biol.*, *29*(2), 259–274.

van Genuchten, M. (1980), A close-form equation for predicting the hydraulic conductivity of unsaturated soils, *Soil Sci. Soc. Am. J.*, *44*(5), 892–898.

Voltz, T., M. Gooseff, A. S. Ward, K. Singha, M. Fitzgerald, and T. Wagener (2013), Riparian hydraulic gradient and stream-groundwater exchange dynamics in steep headwater valleys, *J. Geophys. Res. Earth Surface*, *118*, 953–969, doi:10.1002/jgrf.20074.

Ward, A. S., M. N. Gooseff, and P. A. Johnson (2011), How can subsurface modifications to hydraulic conductivity be designed as stream restoration structures? Analysis of Vaux's conceptual models to enhance hyporheic exchange, *Water Resour. Res.*, *47*, W08512, doi:10.1029/2010WR010028.

Ward, A. S., M. Fitzgerald, M. N. Gooseff, T. J. Voltz, A. M. Binley, and K. Singha (2012), Hydrologic and geomorphic controls on hyporheic exchange during base flow recession in a headwater mountain stream, *Water Resour. Res.*, *48*, W04513, doi:10.1029/2011WR011461.

Ward, A. S., M. N. Gooseff, and K. Singha (2013a), How does subsurface characterization affect simulations of hyporheic exchange?, *Ground Water*, *51*(1), 14–28.

Ward, A. S., M. N. Gooseff, T. J. Voltz, M. Fitzgerald, K. Singha, and J. P. Zarnetske (2013b), How does rapidly changing discharge during storm events affect transient storage and channel water balance in a headwater mountain stream?, *Water Resour. Res.*, *49*, 5473–5486, doi:10.1002/wrcr.20434.

Ward, A. S., M. N. Gooseff, M. Fitzgerald, T. J. Voltz, and K. Singha (2014), Spatially distributed characterization of hyporheic solute transport during baseflow recession in a headwater mountain stream using electrical geophysical imaging, *J. Hydrol.*, *517*, 362–377.

Ward, A. S., N. M. Schmadel, S. M. Wondzell, C. Harman, M. N. Gooseff, and K. Singha (2016), Hydrogeomorphic controls on hyporheic and riparian transport in two headwater mountain streams during base flow recession, *Water Resour. Res.*, *52*, 1479–1497, doi:10.1002/2015WR018225.

Ward, A. S., N. M. Schmadel, S. M. Wondzell, M. N. Gooseff, and K. Singha (2017), Dynamic hyporheic andriparian flow path geometry throughbase flow recession in two headwatermountain stream corridors, *Water Resour. Res.*, *53*, 3523–4526, doi:10.1002/2016WR019875.

Wondzell, S. M. (2006), Effect of morphology and discharge on hyporheic exchange flows in two small streams in the Cascade Mountains of Oregon, USA, *Hydrol. Processes*, *20*(2), 267–287.

Wondzell, S. M., and M. N. Gooseff (2013), 9.13 Geomorphic controls on hyporheic exchange across scales: Watersheds to particles, in *Treatise on Geomorphology*, edited by J. F. Shroder, pp. 203–218, Academic, San Diego, Calif.

Wondzell, S. M., J. LaNier, and R. Haggerty (2009), Evaluation of alternative groundwater flow models for simulating hyporheic exchange in a small mountain stream, *J. Hydrol.*, *364*(1–2), 142–151.

Wörman, A., A. I. Packman, L. Marklund, J. W. Harvey, and S. H. Stone (2007), Fractal topography and subsurface water flows from fluvial bedforms to the continental shield, *Geophys. Res. Lett.*, *34*, L07402, doi:10.1029/2007GL029426.

Zarnetske, J. P., R. Haggerty, S. M. Wondzell, and M. A. Baker (2011), Dynamics of nitrate production and removal as a function of residence time in the hyporheic zone, *J. Geophys. Res.*, *116*, G01025, doi:10.1029/2010JG001356.

Zimmer, M. A., and L. K. Lautz (2014), Temporal and spatial response of hyporheic zone geochemistry to a storm event, *Hydrol. Processes*, *28*(4), 2324–2337.